

## Article

# An Experimental Study on the Impact of the Particle Size and Proportion of Composite Proppant on the Conductivity of Propped Fractures in Coalbed Methane Reservoirs following Pulverized Coal Fines Infiltration

Qing Chen <sup>1,2</sup>, Zhiqiang Huang <sup>1,2,\*</sup>, Hao Huang <sup>1,2,\*</sup>, Qi Chen <sup>1,2</sup>, Xingjie Ling <sup>1,2</sup>, Fubin Xin <sup>1,2</sup> and Xiangwei Kong <sup>1,2</sup>

<sup>1</sup> Petroleum Engineering College, Yangtze University, Wuhan 430100, China; 2022730010@yangtzeu.edu.cn (Q.C.)

<sup>2</sup> National Engineering Research Center for Oil & Gas Drilling and Completion Technology, Wuhan 430100, China

\* Correspondence: huangzq@yangtzeu.edu.cn (Z.H.); 2022730022@yangtzeu.edu.cn (H.H.)

**Abstract:** Coalbed methane reservoirs exhibit a low strength and high heterogeneity, rendering them susceptible to coal fines generation during hydraulic fracturing operations. The detrimental impact of coal fines on the conductivity of the propped fracture has been overlooked, leading to a substantial negative effect on the later-stage recovery of coalbed methane reservoirs. Moreover, the particle size distribution of the composite proppant also affects the conductivity of the propped fracture. To mitigate the damage caused by coal fines to the conductivity of the proppant pack in CBM reservoirs, this study conducted conductivity tests on actual coal rock fractures. The aim was to assess the effect of various particle size ratios in composite proppant blends on the conductivity of complex fractures in CBM reservoirs. The ultimate goal was to identify an optimized proppant blending approach that is suitable for hydraulic fracturing in coal seams. The results indicated that, in terms of the short-term conductivity of coalbed methane reservoirs, the conductivity of composite proppants is primarily influenced by the proportion of large or small particles. A higher proportion of large particles corresponds to a stronger conductivity (e.g., the conductivity is highest at a particle ratio of 5:1:1 for large, medium, and small particles). On the other hand, a higher proportion of small particles leads to a poorer conductivity (the conductivity is lowest when the particle ratio is 1:1:5). In the long-term conductivity of coalbed methane reservoirs, the fluid flushing of the fracture surfaces generates coal fines, and small particles can fill the gaps between larger particles, hindering the infiltration of coal fines. Therefore, it is important to control the particle size ratio of composite proppants, with a predominant proportion of larger particles. This approach can maintain long-term conductivity and prevent the excessive infiltration of coal fines, thereby avoiding fracture blockage (e.g., the conductivity is highest at a particle ratio of 5:1:5, followed by a ratio of 3:1:3). Furthermore, considering the influence of proppant placement methods and the support effect on near-wellbore opening fractures and far-end sliding fractures, segmented placement is utilized to fully fill the fractures for short-term conductivity, whereas mixed placement is employed for long-term conductivity to achieve a balance in particle gaps and hinder the infiltration of coal fines. The findings of this study contribute to the understanding of proppant selection and placement strategies for efficient hydraulic fracturing in coalbed methane reservoirs.

**Keywords:** coalbed methane reservoir; composite particle size proppant; particle ratio; propped fracture; conductivity



**Citation:** Chen, Q.; Huang, Z.; Huang, H.; Chen, Q.; Ling, X.; Xin, F.; Kong, X. An Experimental Study on the Impact of the Particle Size and Proportion of Composite Proppant on the Conductivity of Propped Fractures in Coalbed Methane Reservoirs following Pulverized Coal Fines Infiltration. *Processes* **2023**, *11*, 2205. <https://doi.org/10.3390/pr11072205>

Academic Editor: Qingbang Meng

Received: 7 June 2023

Revised: 16 July 2023

Accepted: 21 July 2023

Published: 22 July 2023



**Copyright:** © 2023 by the authors. Licensee MDPI, Basel, Switzerland. This article is an open access article distributed under the terms and conditions of the Creative Commons Attribution (CC BY) license (<https://creativecommons.org/licenses/by/4.0/>).

## 1. Introduction

Coalbed methane (CBM) is highly valued as a new clean energy source and high-quality chemical raw material due to its abundant reserves, low cost, and clean efficiency [1].

The development of CBM has garnered significant attention from various countries, with a primary focus on low-rank coal in countries such as the United States and Australia. Conversely, China possesses complex CBM resources with a relatively higher gas content. However, as the depth of CBM development increases, and coal permeability remains low, the production of CBM becomes constrained. Hydraulic fracturing is essential to enhancing the productivity of CBM wells. However, due to its lower compressive and tensile strength, as well as the development of cleats, coal rock exhibits brittleness, a susceptibility to collapse, and the generation of coal fines. Compared to conventional reservoirs, coal rock is more susceptible to mechanical damage and stress alteration during the hydraulic fracturing process. As a result, a large amount of coal fines become dislodged and accumulate, contaminating the proppant. The transportation and retention of coal fines in the proppant pack lead to the blockage of the fluid pathways within the coalbed, reducing the fracture conductivity and subsequently decreasing the production capacity of CBM [2–6]. Furthermore, the infiltration of coal fines into the pump barrel can cause pump sticking, blockage, equipment damage, and even production shut-in, posing severe hazards. Current research has indicated that the presence of coal fines is one of the primary factors limiting the efficiency of CBM production [7–10]. Therefore, investigating the production and transport behavior of coal fines and implementing measures to control their accumulation are crucial for achieving the efficient and stable extraction of CBM [11]. Addressing the current technical challenges of low productivity in high-rank CBM reservoirs, mitigating the detrimental effects of coal fines on the conductivity of coalbed hydraulic fracturing propped fractures [12,13], and formulating rational CBM extraction strategies would advance the CBM industry [14].

The detachment and transport of coal fines can significantly reduce the permeability of the CBM reservoir fracture system. Several researchers have conducted studies on the transport of coal fines. Wang Hanxiang et al. [15] investigated the influence of coal rock deformation, detachment, transport, and the deposition of coal fines in fractures, as well as pore throat blockage, on the physical parameters of coal rock. They developed a mathematical model for the two-phase flow of coal fines and fluid. Zhang Fenna et al. [16] developed a model for the suspended transport of coal fines, incorporating the principle of moderate sand production in oil and gas fields, and proposed a new approach for the moderate discharge of coal fines. Li Yong et al. [17] summarized the research progress on the coagulation-settlement-dispersion of coal fines, identified unresolved issues in coal fines research, and provided research directions for effective coal fines production and the efficient development of CBM. In numerical simulation studies, Zheng Chunfeng et al. [18] investigated the transport characteristics of coal fines in the wellbore during CBM production. They found that a higher initial velocity of the solid–liquid two-phase flow resulted in a closer flow rate between the coal fines particles and the drilling fluid, facilitating the discharge of the coal fines. Zhang Jian et al. [19] analyzed the impact of coal fines transport at different stages on CBM production using a numerical simulation. In experimental studies, Liu Yan et al. [20] conducted physical simulation experiments to examine the influence of flow rates and coal fines content on the conductivity of propped fractures. They investigated the critical flow rate of the coal fines transport under varying conditions and analyzed the patterns of the transport and deposition of the coal fines in the propped fractures. Chen Wenwen et al. [21] conducted simulation experiments using transparent tubes to investigate coal fines detachment, transport, and production. They examined the effects of fluid velocity, medium type, and coal fines particle size on the transport and production of coal fines, and proposed engineering measures to control the coal fines production in CBM wells. Zhao Shuai et al. [22] conducted a series of experiments, including a microscopic model simulation, API conductivity experiments, and gas–water phase seepage experiments, to investigate the characteristics of coal fines transport and blockage, as well as their influencing factors, during the simultaneous flow of coal fines, microbubbles, and water.

Furthermore, numerous scholars have conducted extensive experimental research on the factors influencing the conductivity of propped fractures in hydraulic fracturing [23–27]. Cao Kexue et al. [28] conducted experiments on the conductivity of quartz sand and ceramic composite proppants and optimized the proppant selection for field fracturing designs under a closure pressure of 25–35 MPa. Li Yuwei et al. [29] conducted experimental research to investigate the long-term conductivity of complex coal rock fractures. They examined the impact of coal rock fracture complexity under different testing conditions on conductivity. Liang Tiancheng et al. [30] analyzed the performance and short-term flow capacity of different proppants using a large amount of indoor evaluation test data, studying the primary controlling factors that influenced conductivity. Zhao Zhenfeng et al. [31] conducted experimental research to investigate the influence of quartz sand proppants on the long-term conductivity of propped fractures and proposed a predictive model for estimating this conductivity based on proppant mixed placement. Jin Ping et al. [32] analyzed the impact of different factors on the conductivity of fracture networks in tight sandstone reservoirs through hydraulic fracture conductivity testing experiments. Chen Chi et al. [33] conducted multi-scale fracture conductivity experiments using exposed rock cores to investigate the influencing patterns on the fracture conductivity. Zhu Huajun et al. [34] conducted fracture flow capacity testing experiments with different types, sizes, and combinations of proppants to investigate the influence of proppant particle size combinations on conductivity. Zhang Hongjun et al. [35] conducted fracture flow capacity testing experiments with improved proppant packs to investigate the impact of proppant particle size, proppant concentration, coal rock elastic modulus, coal fines content, and fracturing fluid type on the conductivity of complex coal rock fractures. Ren Lan et al. [36] conducted fracture conductivity experiments under high closure stress conditions in deep shale formations to evaluate the effectiveness of deep shale gas fracturing networks. Xiao Fengchao et al. [37] established a dense, discrete-phase model for proppant particle size distribution, studied the proppant transportation and placement patterns in the main fractures, and conducted indoor conductivity evaluation experiments.

Studies have also been conducted to investigate the impact of coal fines on the conductivity of propped fractures in coalbed hydraulic fracturing. Wang Changhao et al. [38] conducted experiments on the conductivity of sand-filled fractures in coal, investigating the influence of coal fines particle size on the fracture conductivity. Zou et al. [39] conducted experiments on the migration of coal fines within propped fractures, analyzing the impact of dispersants on the damage pattern of coal fines to the fracture permeability. Yang Yu et al. [40] investigated the formation mechanism of coal fines during hydraulic fracturing, their impact on CBM reservoirs, and proposed measures to mitigate the damage caused by coal fines migration. Liu Yan et al. [41] performed conductivity tests to examine the influence and damage mechanism of coal fines on the fracture conductivity at various flow rates. Ahamed et al. [42] investigated the influence of closure pressure and proppant types on the conductivity of propped fractures in coalbed hydraulic fracturing. Liu Ziliang et al. [43] conducted physical simulation experiments using coal rock samples collected from the field to investigate the influence of different water chemistry properties on coal fines transport in propped fractures. They analyzed the relationship between the fracture conductivity and the concentration of the coal fines produced.

The aforementioned studies primarily investigated the conductivity of propped fractures in sandstone and shale reservoirs, with a particular focus on analyzing the impact of various factors. These factors encompass the type, particle size, and combination of proppants. However, there is a research gap in understanding the correlation between proppant particle size combinations, coal fines content, and the conductivity of propped fractures. The particle size combination of proppants also plays an important role in reducing the damage caused by coal fines to the conductivity of propped fractures.

This study aims to identify the proppant particle size combinations that can prevent the infiltration of coal fines and mitigate their damage to the conductivity of propped fractures. This objective will be achieved through coal rock conductivity testing experi-

ments. The experimental materials were prepared in accordance with the standards set by the petroleum and natural gas industry. Standard rough diversion coal rock slabs were prepared by processing coal rock outcrops from Well S-1 in the Shizhuang block. These rock slabs were designed to replicate the morphology of actual underground CBM reservoir fractures. Ceramic proppants with particle sizes of 30 mesh, 60 mesh, and 90 mesh, which conform to industry standards, were chosen to represent large, medium, and small particles, respectively. The conductivity testing experiments were then conducted using proppants of single-particle sizes, as well as proppants with different ratios of two and three particle sizes. The experiments assessed the influence of various closure pressures and particle size ratios on the short-term and long-term conductivity of the CBM reservoir. Additionally, the benefits of proppants with varying particle size ratios in relation to the short-term and long-term conductivity in the coal rock were analyzed. Lastly, the study discussed the capability of proppants with different particle size ratios to hinder the infiltration of coal fines. The goal was to optimize the composite proppant particle size ratios suitable for coalbed fracturing and enhance the conductivity of the propped fractures. The main innovation of this study is the comprehensive examination of proppant particle size ratios and the impact of coal fines on the conductivity in CBM reservoirs. The research findings will offer valuable guidance for the design of hydraulic fracturing in CBM reservoirs, thereby enhancing CBM production and optimizing the development of CBM.

## 2. Experimental Study on Conductivity of Coalbed Propped Fractures

### 2.1. Experimental Apparatus

Figure 1 depicts the schematic diagram of the experimental setup used to assess the conductivity of proppants in CBM reservoirs. The experimental method for evaluating the conductivity of these propped fractures in CBM reservoirs during hydraulic fracturing adhered to the industry standard SY/T6302-2009, titled “Recommended Method for Evaluating the Short-Term Conductivity of Proppant Pack”. The experimental equipment included a linear conductivity test cell adhering to API standards, a hydraulic press with a pressure compensation system, a core holder, a displacement apparatus for experimental liquid, flowmeters, pressure differential gauges, pressure sensors, and a backpressure-regulating device. By introducing composite proppants comprising different particle sizes and ratios, the study simulated the conductivity of propped fractures under various closure stresses, and subsequently conducted conductivity tests.

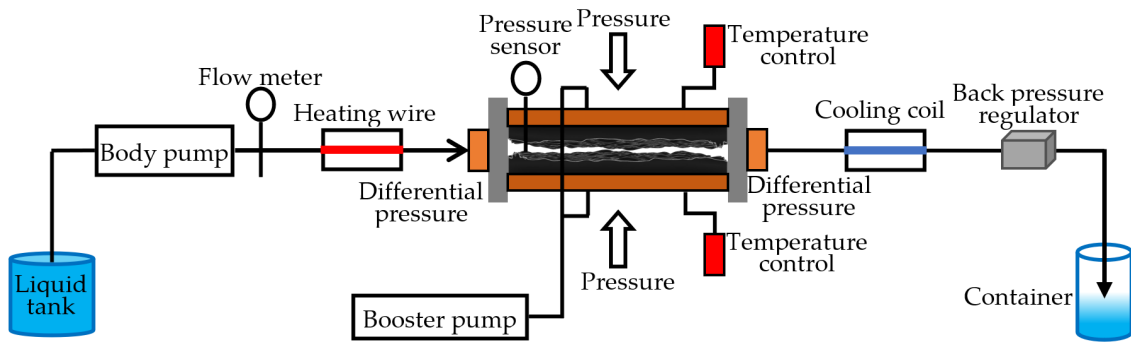
### 2.2. Experimental Principles

As shown in Figure 2, the areas of the adjacent gaps between the single-sized proppants (with a particle radius  $r_1$ ), two-sized proppants (with particle radii  $r_1$  and  $r_2$ ), and three-sized proppants (with particle radii  $r_1$ ,  $r_2$ , and  $r_3$ ) followed this order:  $A_1 > A_2 > A_3$ . Smaller particle gaps are less prone to being filled by coal fines. Additionally, as the closure pressure increases, the gaps between the proppant particles shrink, enabling coal fines to infiltrate these gaps, thereby further reducing the conductivity of the propped fractures. Figure 3's schematic diagram illustrates the deformation of the proppant under compression. Leveraging this characteristic, experiments were conducted to optimize the particle size ratios of the composite proppants, aiming to effectively enhance the conductivity of the propped fractures in CBM reservoirs.

The experimental principle adheres to Darcy's law, which enables the calculation of the permeability of a propped fracture using the following equation:

$$K_f = \frac{Q_f \mu L}{A \Delta p} \quad (1)$$

where  $K_f$  is the permeability of the propped fracture in  $\mu\text{m}^2$ ;  $Q_f$  is the flow rate within the fracture in  $\text{cm}^3/\text{s}$ ;  $\Delta p$  is the pressure difference across the ends of the fracture in MPa;  $\mu$  is the viscosity of the experimental fluid in  $\text{mPa}\cdot\text{s}$ ; and  $A$  is the cross-sectional area of the propped fracture in  $\text{cm}^2$ .



(a) Schematic diagram of the experimental setup



(b) The physical picture of the experimental device

Figure 1. Schematic diagram of experimental setup for proppant conductivity in coal rock reservoir.

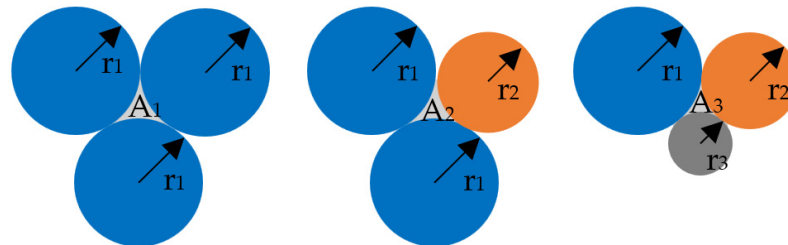


Figure 2. Characteristics of adjacent gaps between single particle size and composite particle size proppants.

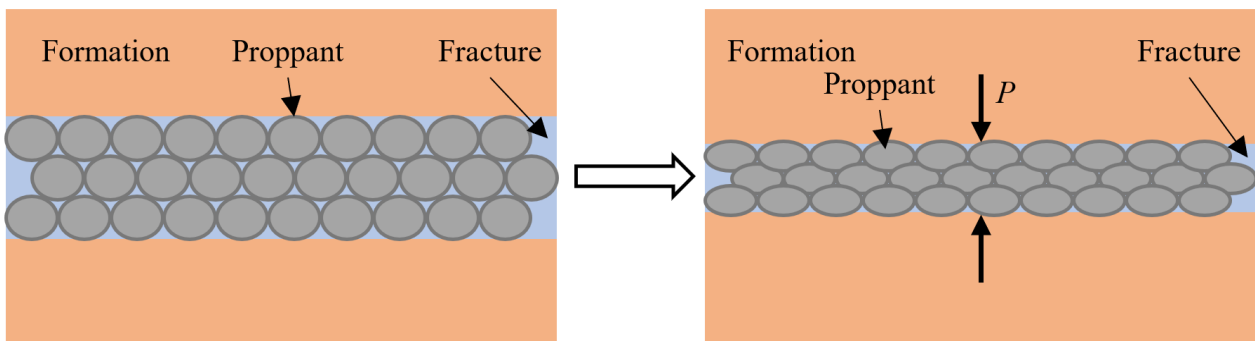


Figure 3. Schematic diagram of proppant compression deformation.

The fracture flow system employed an API standard linear flow cell with dimensions of 12.7 cm (length) and 3.81 cm (width). The experimental setup involved a rough fracture with

a filling layer thickness equal to the fracture's average width. The formula for calculating the permeability of the propped fracture can be expressed as follows:

$$K_f = \frac{12.7Q\mu}{w\bar{h}\Delta p} \quad (2)$$

where  $w$  is the width of the proppant-filled layer, cm; and  $\bar{h}$  is the thickness of the proppant-filled layer, cm.

The conductivity is determined as follows:

$$P = \frac{12.7Q\mu}{w\Delta p} \quad (3)$$

where  $P$  is the flow capacity of the propped fracture, expressed as  $\mu\text{m}^2\cdot\text{cm}$ .

### 2.3. Experimental Preparation

#### 2.3.1. Experimental Materials

The experimental rock samples were collected from the coal rock outcrop in the Shizhuang block. They were cut and processed to create a rough coal rock slab (Figure 4), with dimensions of 12.7 cm (length), 3.81 cm (width), and 3 cm (thickness). The slab had a square end and the rough topography of the internal fracture was obtained through Brazilian splitting. The rock samples were clamped and positioned inside the flow chamber, with supporting agents being placed between the internal fractures for the conductivity testing. The fracture width was determined following the industry standard SY/T6302-2009, titled "Recommended Method for Evaluating Short-Term Conductivity of Fracturing Proppant Packs." A minimum fill width of 0.25 cm was selected, and three particle size ranges were chosen: 850  $\mu\text{m}$  to 425  $\mu\text{m}$ , 600  $\mu\text{m}$  to 300  $\mu\text{m}$ , and 425  $\mu\text{m}$  to 212  $\mu\text{m}$ .



**Figure 4.** Illustration of a rough coal-rock slab.

The experiment utilized ceramic proppants known for their low crushing rate. This feature prevented particle breakage, which could otherwise disrupt the infiltration pattern of the coal fines and impact the experimental results. Three particle size ranges (30 mesh, 60 mesh, and 90 mesh) were designated for the proppants. The preparation of the proppants adhered to the guidelines specified in SY/T5108-2014, titled "Performance Testing Method for Proppants Used in Hydraulic Fracturing and Gravel Packing Operations". The proppants underwent evaluation and were found to meet industry standards. Their fundamental performances are presented in Table 1.

**Table 1.** Basic performance of experimental proppants.

Proppant Type	Particle Size/Mesh	Density /( $\text{g}\cdot\text{cm}^{-3}$ )	Average Particle Size / $\mu\text{m}$	Roundness/Sphericity	Turbidity
Ceramic proppant	30 (Large particle)	2.31	713.26	0.9/0.9	62.3
	60 (Medium particle)	2.32	376.51	0.9/0.9	63.5
	90 (Small particle)	2.31	168.74	0.9/0.9	61.7
	Industry standard requirements			$\geq 0.7/\geq 0.7$	$\leq 100$

### 2.3.2. Design of Proppant Placement Patterns

Figure 5 illustrates the utilization of three different proppant placement methods. In the figure, blue represents the large-sized proppant, orange represents the medium-sized proppant, and black represents the small-sized proppant. Figure 5a depicts the uniform placement of a single-sized proppant. Figure 5b demonstrates the uniform mixture placement of the two different sized proppants. Figure 5c exhibits the uniform mixture placement of the three different sized proppants. The conductivity testing experiments were carried out using predetermined proppant combination patterns. These patterns included single-sized proppants (30 mesh, 60 mesh, and 90 mesh), medium–small-sized proppant combinations (30/60 mesh, 60/90 mesh, and 30/90 mesh with varying ratios), and large–medium–small-sized proppant combinations (30/60/90 mesh with varying ratios), aiming to evaluate their conductivity.

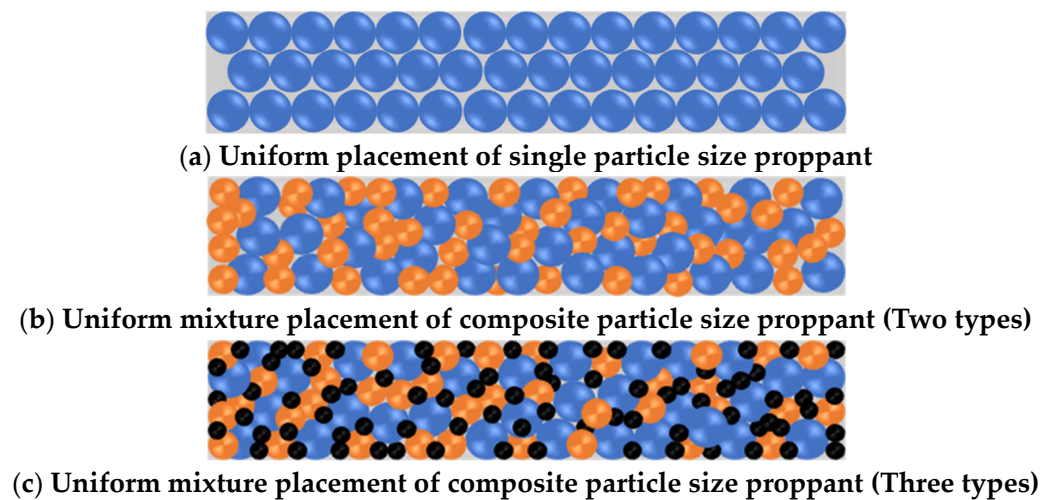


**Figure 5.** Schematic diagram of placement patterns of proppants with different particle sizes.

### 2.4. Design of Proppant Placement Patterns

Hydraulic fracturing generates hydraulic fractures, including tensile-induced opening fractures near the wellbore and shear-induced sliding fractures at the far end. These fractures vary in scale and necessitate the appropriate placement to effectively fill and support the entire fracture network. Therefore, considering the compatibility between different sized proppants and fractures of varying scales is crucial. Optimizing the particle size ratio of the composite proppants is particularly important in coalbed hydraulic fracturing, as the mixture of coal fines and proppants can readily obstruct the fractures and impact the conductivity of the propped fractures. The experiments involved collecting coal rock samples from the field to replicate an authentic underground coalbed hydraulic fracturing environment. Analytical experiments were then performed to analyze the conductivity of the composite proppants with different sizes. Each experiment was repeated three times, and the results presented represent the average values of each experimental group. The specific design scheme is depicted in Figure 6, while Figure 7 illustrates the schematic diagram of the flow chamber and the flow testing of the propped fractures.

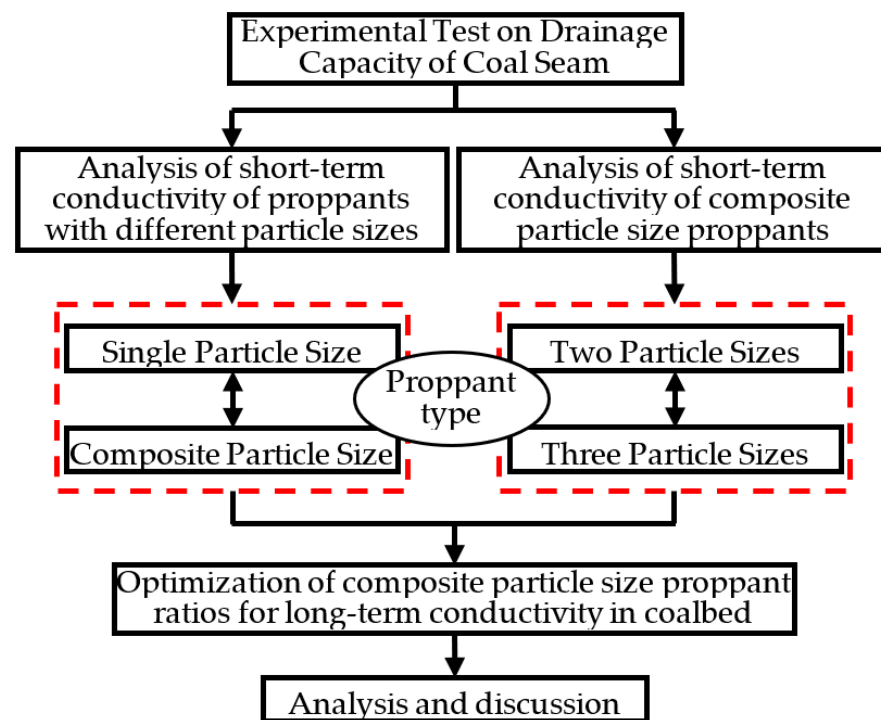


Figure 6. Experimental design for conductivity of propped fractures.

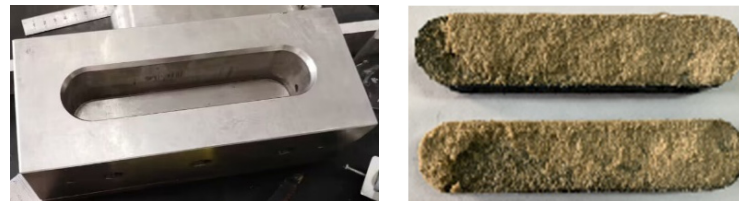
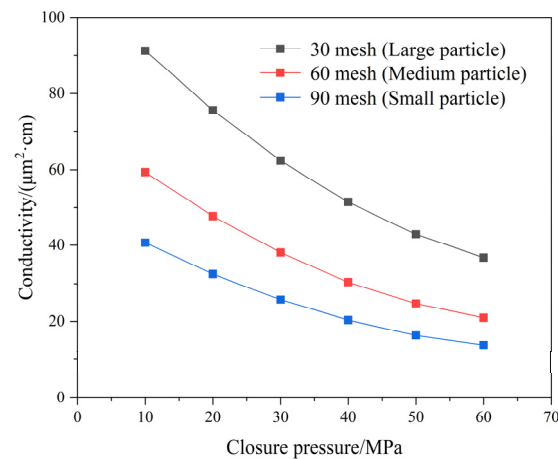


Figure 7. Diversion chamber and propped fractures conductivity test chart.

### 3. Analysis of Experimental Results

#### 3.1. Influence of Single Particle Size on Short-Term Conductivity of Coalbed Propped Fractures

The experiment compared the short-term conductivity of single-sized proppants with particle sizes of 30 mesh, 60 mesh, and 90 mesh under various closure pressures. The experimental results are presented in Figure 8, which shows that, under constant conditions, the conductivity of the propped fractures increased gradually with larger proppant particle sizes. At a closure pressure of 10 MPa, the conductivity values for the proppants with particle sizes of 90 mesh, 60 mesh, and 30 mesh were  $40.67 \mu\text{m}^2\cdot\text{cm}$ ,  $59.36 \mu\text{m}^2\cdot\text{cm}$ , and  $91.23 \mu\text{m}^2\cdot\text{cm}$ , respectively. These results demonstrate a stepwise increasing trend. However, as the closure pressure increased, the conductivity of the propped fractures gradually decreased due to increased proppant compaction within the fracture, resulting in reduced gaps between the proppant particles and affecting their overall conductivity. Notably, at a closure pressure of 60 MPa, the decrease in conductivity became more gradual, indicating that the gaps between the proppant particles were already significantly small, and the compaction level of the proppants decreased, assuming no particle crushing occurred.



**Figure 8.** Short-term conductivity variation with closure pressure for different particle size proppants.

Figure 9 presents a heat map illustrating the relationship between the conductivity of the propped fractures and the closure pressure, as well as the particle size, based on the aforementioned results. The figure reveals that the conductivity was directly proportional to the proppant particle size and inversely proportional to the closure pressure. In simpler terms, a larger proppant particle size and lower closure pressure led to a higher conductivity of the propped fractures. Under the present experimental conditions, the propped fractures exhibited their maximum conductivity at a closure pressure of 10 MPa and a particle size of 300  $\mu\text{m}$ , measuring 52.4  $\mu\text{m}^2\cdot\text{cm}$ . Conversely, the propped fractures demonstrated their minimum conductivity at a closure pressure of 60 MPa and a particle size of 50  $\mu\text{m}$ , measuring 5.6  $\mu\text{m}^2\cdot\text{cm}$ .

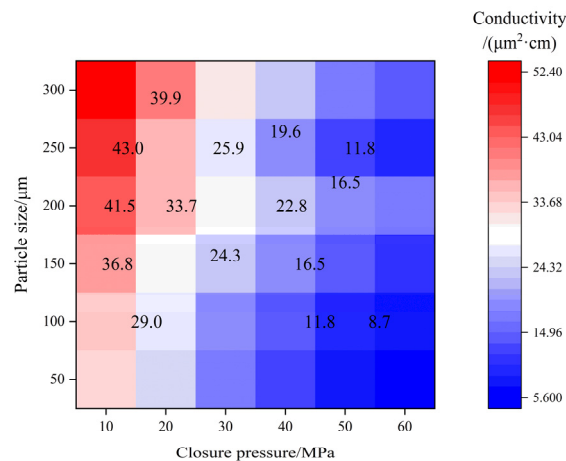


**Figure 9.** Heatmap of conductivity variation with closure pressure and particle size in propped fractures.

This results indicate that the conductivity of the coalbed propped fractures was minimally affected under different closure pressure conditions during short-term diversion with a low coal fines content. In such a situation, employing larger-sized proppants can effectively enhance the conductivity of propped fractures. However, in practical field applications, when selecting the proppant size, the width of the far-end sliding fractures [33] needs to be considered. These fractures are depicted in Figure 10. The fracture network formed by hydraulic fracturing consists of tensile fractures near the wellbore caused by tensile forces, as well as numerous non-matching shear slip fractures that extend to the far end of the hydraulic fracturing zone and exhibit shear displacement movement. They develop away from the injection point and typically intersect or nearly intersect with the main fractures. The distal shear slip fractures are often secondary fractures generated

during the hydraulic fracturing process and interact with the main fractures. However, if the particle size is excessively large, the proppants will be unable to fully fill the fractures, leading to incomplete and ineffective support of the fractures, which significantly impairs the conductivity after fracture propping.

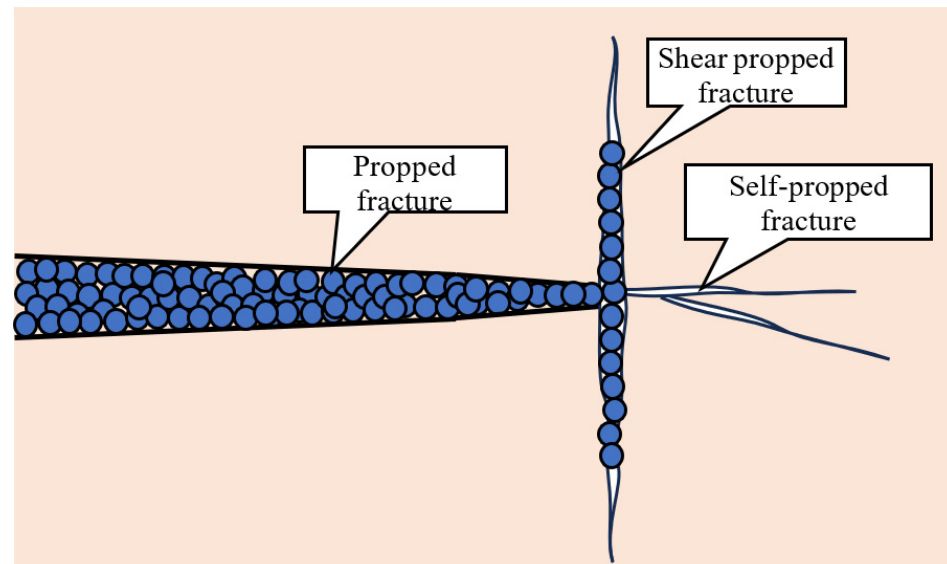


**Figure 10.** Multi-level fracture body formed after pressing.

### 3.2. Influence of Composite Particle Sizes on Short-Term Conductivity of Coalbed Propped Fractures

Filling small-scale fractures with large-sized proppants is not feasible due to the size disparity between the open fractures near the wellbore and the sliding fractures at the far end. As a result, using small-sized proppants does not fully leverage the conductivity of the propped fractures. To address the challenge of achieving comprehensive filling, the conductivity of the two-component/three-component composite proppants was assessed and analyzed based on the propped fracture conductivity.

#### 3.2.1. Influence of Two Particle Sizes Composite Proppant

Figure 11 presents a comparison of the short-term conductivity among the two-component composite proppants with particle sizes of 30 mesh, 60 mesh, and 90 mesh under varying closure pressures. The graph reveals that, at an identical closure pressure, the composite proppants with the same particle size ratio exhibited a decreasing conductivity in the following sequence: 30/60 mesh, 30/90 mesh, and 60/90 mesh. With an increasing closure pressure, the conductivity of the composite proppants demonstrated three distinct decreasing trends, with the strength of the conductivity following a consistent pattern. These three types of composite proppants can be categorized based on their decreasing conductivity as follows: 30/60 mesh (5:1), 30/90 mesh (5:1), 30/60 mesh (3:1), 30/90 mesh (3:1), and 30/60 mesh (1:1), constituting one category; 30/90 mesh (1:1), 60/90 mesh (5:1), 60/90 mesh (3:1), 30/60 mesh (1:3), and 30/90 mesh (1:3) falling into another category; and 30/60 mesh (1:5), 30/90 mesh (1:5), 60/90 mesh (1:1), 60/90 mesh (1:3), and 60/90 mesh (1:5) making up a third category. The proportion of larger particles gradually decreased across these three categories.

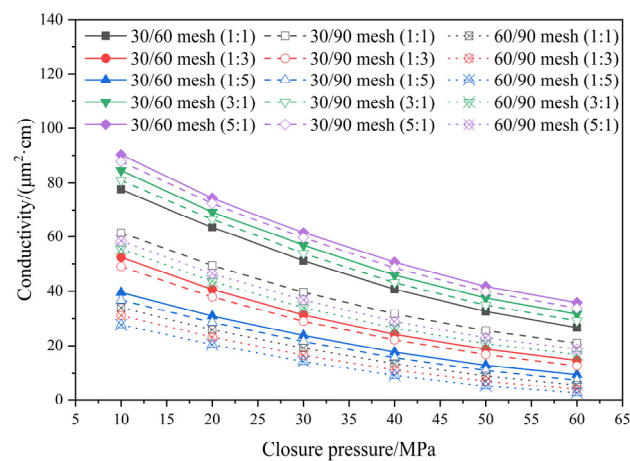


**Figure 11.** Influence of uniform/non-uniform ratio of composite particle size proppants on short-term conductivity (Two particle sizes).

This indicates that, as the closure pressure increased, the proppant particles in the propped fracture underwent compaction, leading to a gradual decrease in the particle spacing and a reduction in the conductivity of the propped fracture. Furthermore, a smaller average particle size resulted in a lower individual particle compression and weaker compaction, leading to a slower decrease in conductivity. It is noteworthy that smaller particles demonstrated a greater resistance to compression.

The proportion of a particular particle size within the composite proppant gradually approached the conductivity of a single particle size. A higher proportion of larger particles corresponded to a stronger conductivity, whereas a higher proportion of smaller particles resulted in a weaker conductivity. For instance, at the same closure pressure, the conductivity was strongest for the 30/90 mesh (5:1) composite proppant, while it was lowest for the 60/90 mesh (1:5) composite proppant. Furthermore, the composites containing larger and intermediate particles clearly demonstrated a significantly stronger conductivity in comparison to those comprising intermediate and smaller particles.

In summary, a larger particle size or a higher proportion of larger particles resulted in a stronger conductivity but a lower resistance to compression. Therefore, as the closure pressure increased, the decrease in conductivity became more pronounced. When diverting for short-term purposes under different closure pressure conditions, the optimal choice was to utilize composite proppants with particle size ratios of 30/60 mesh (5:1), 30/60 mesh (3:1), or 60/90 mesh (5:1). These composite proppants, comprising large and medium particles, large and small particles, or medium and small particles, were chosen to support the fractures, thereby minimizing the damage to the conductivity of the propped fractures. Moreover, small particles should be suitably configured to effectively fill the open fractures near the wellbore and the sliding fractures at the far end, thereby preventing fracture closure and minimizing the impact on CBM production. However, achieving the comprehensive and uniform filling of the entire fracture channel may be challenging due to the limited range of particle sizes in the two-component gradation. Further exploration is required to fully understand the benefits of different graded proppants.

### 3.2.2. Influence of Three Particle Sizes Composite Proppant

The design scheme for testing the short-term conductivity of the composite proppants with three different particle sizes is presented in Table 2. The experiment evaluated the short-term conductivity of the composite proppants with varying ratios of 30 mesh, 60 mesh, and 90 mesh at different closure pressures, as depicted in Figure 12.

**Table 2.** Design of ratio for testing short-term conductivity of three particle sizes composite proppants.

Experimental Number	30/60/90 Mesh Uniform Ratio (Control Group)	30/60/90 Mesh Non-Uniform Ratio (EXPERIMENTAL Group)	Experimental Content
1	1:1:1	1:1:3, 1:1:5	The influence of the density of large, medium, or small particles on the conductivity.
2		1:3:1, 1:5:1	
3		3:1:1, 5:1:1	
		1:3:3, 1:5:5	The impact of uniform ratio of two particle sizes on the conductivity.
		3:1:3, 5:1:5	
		3:3:1, 5:5:1	
		1:3:5, 1:5:3	The impact of non-uniform ratio of three particle sizes on the conductivity.
		3:1:5, 5:1:3	
		3:5:1, 5:3:1	
Objective	Optimal ratio for the combination of large, medium, and small particles		

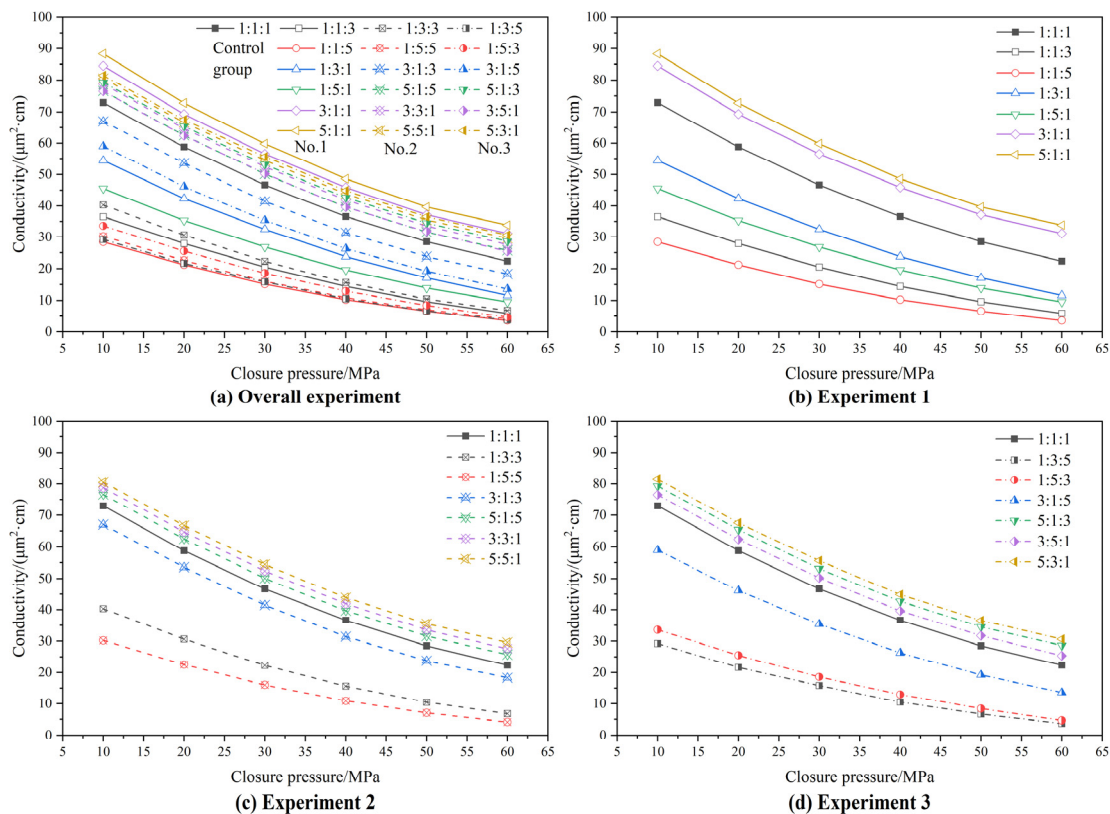


**Figure 12.** Influence of uniform/non-uniform ratio of composite particle size proppants on short-term conductivity (Three particle sizes).

The conductivity curves of all the experimental results in Figure 12a show a hierarchical pattern characterized by dense-sparse-dense. The proportion of large and small particles had a polarizing effect on the conductivity of the proppant. A higher proportion of large particles resulted in a stronger conductivity but a larger decline. Conversely, a higher proportion of small particles resulted in a poorer conductivity but a smaller decline. Changes in the proportion of the medium particles resulted in a polarization phenomenon in their conductivity, as they simultaneously affected the quantities of large and small particles.

In Experiment 1, Figure 12b shows that an increase in the proportion of large particles in the composite proppant enhanced the conductivity. Conversely, a higher proportion of small particles resulted in a poorer conductivity. Additionally, an increase in the proportion of medium particles led to a decrease in conductivity, due to the reduced number of large particles, which was affected the within the fractures.

Figure 12c shows that, in Experiment 2, as the proportions of both the large and medium particles uniformly increased, a higher proportion of large and medium particles resulted in a stronger conductivity. Conversely, a higher proportion of medium and small particles led to a poorer conductivity. However, an increase in the proportion of both large and small particles resulted in conductivity due to the presence of more small particles that impeded the conductivity in the gaps filled by large particles.

Figure 12d shows that, in Experiment 3, an uneven increase in the proportions of both large and medium particles resulted in an enhanced conductivity, with a greater impact when there were more large particles. Conversely, a higher proportion of medium and small particles resulted in a reduced conductivity, with a greater impact when there were more small particles. Additionally, an increase in the proportion of both large and small particles resulted in a stronger conductivity, with a greater impact when there were more large particles.

The proportions of large and small particles were the main factors influencing the conductivity of the proppant in the three mentioned experiments under different ratios. A higher proportion of large particles resulted in a stronger conductivity, whereas a smaller proportion of small particles led to a poorer conductivity. However, an increase in the proportion of medium particles reduced the quantity of the large particles, thereby reducing the conductivity of the proppant. Therefore, under different closure pressure conditions, the optimal choice for the short-term conductivity and comprehensive filling of hydraulic fractures is a composite proppant with three particle sizes, such as 30/60/90 mesh (5:1:1), 30/60/90 mesh (3:1:1), or 30/60/90 mesh (5:3:1). This means selecting a particle size ratio for the composite proppant that has a dominant proportion of large particles and a secondary proportion of medium and small particles to support the fractures. This approach ensures minimal damage to the conductivity of the proppant and effectively distributes medium and small particles to effectively fully fill the near-wellbore open fractures and far-end sliding fractures, preventing the closure of the far-end fractures and maximizing the CBM production. For efficient proppant filling, it is recommended to use the 30/60/90 mesh (3:1:1) or 30/60/90 mesh (5:3:1) ratio and implement a segmented and uniform placement method. The particle size placement should start with filling small particles in the far-end small-scale fractures, followed by medium particles, and finally filling large particles in the near-wellbore section.

In conclusion, a greater variety of particle size distribution in the proppant is crucial for efficient fracture filling while minimizing the damage to the conductivity of the proppant. However, the particle size distribution should not be excessive, to prevent the overfilling of the particle gaps.

### *3.3. Influence of Composite Particle Sizes on Long-Term Conductivity of Coalbed Propped Fractures*

Coalbed hydraulic fracturing operations are characterized by the low strength and high heterogeneity of coalbeds, which make them susceptible to the generation of coal fines. With an increasing compaction time, the fluid continuously flushes the fracture surfaces, leading to a growing concentration of coal fines. When combined with the proppant, these fines can easily obstruct the fluid flow channels within the propped fractures, resulting in a decrease in conductivity. Therefore, based on the established benefits of large particles and particle size distribution for conductivity, it is essential to assess the influence of the compaction time on the conductivity of proppants with varying sizes and investigate the composite proppant types that minimize this impact on conductivity in coalbed propped fractures. The object of this research is to improve the post-fracturing gas production in coalbeds. The experimental design scheme outlined in Table 2 was utilized to perform the long-term conductivity tests and investigate the impact of coal fines on the conductivity of the propped fractures. Furthermore, the optimization of the particle size ratios for the composite proppants in coalbed propped fractures was examined. The experimental findings are depicted in Figure 13.

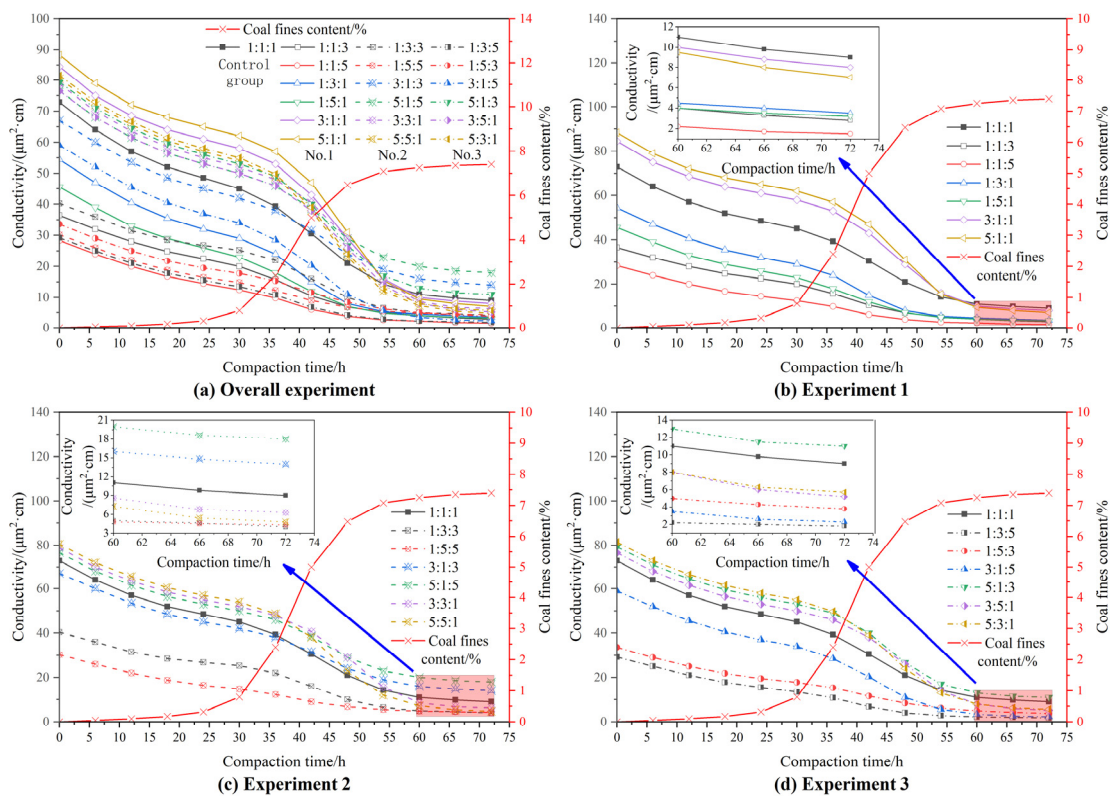


**Figure 13.** Influence of uniform/non-uniform ratio of composite particle size proppants on long-term conductivity (Three particle sizes).

Based on Figure 13a, during the initial stages of the experiments, the conductivity curves of all the results demonstrated a dense-sparse-dense pattern, which aligns with the observations in Figure 12a. However, with an increasing compaction time, the fluid continuously flushed the fracture surfaces, leading to a progressive buildup of coal fines within the propped fractures and a rapid decline in conductivity. This trend persisted until all the coal fines were detached, ultimately leading to a stabilized conductivity.

According to Figure 13b, in Experiment 1, under prolonged compaction, an increased proportion of any particle in the composite proppant led to a decrease in the final conductivity of the propped fractures. This was because a higher proportion of large and medium particles resulted in a reduction in small particles, creating larger particle gaps that allowed for the easier infiltration of coal fines and adversely affected the final conductivity of the propped fractures. Conversely, a higher proportion of small particles reduced the particle gaps, preventing the excessive infiltration of coal fines but also reducing the conductivity of the propped fractures.

Figure 13c reveals that, in Experiment 2, under prolonged compaction, an increased proportion of both particle sizes led to a lower final conductivity of the propped fractures, with a higher proportion of large and medium particles contributing to the decline. This was because the larger particle gaps allowed for a significant infiltration of coal fines, leading to the impairment of the conductivity of the propped fractures. Conversely, a higher proportion of medium and small particles led to a decrease in the final conductivity. However, when the ratio was 1:5:5, there was a slight improvement in the conductivity compared to the 1:3:3 ratio. The slightly higher proportion of small particles reduced the overall particle gap within the fracture, to some extent impeding the excessive infiltration of the coal fines and alleviating the impairment of the conductivity. Additionally, a higher proportion of both large and small particles resulted in a higher final conductivity. The increased presence of large particles was balanced by the increased number of small

particles, which helped to maintain an optimal particle gap and prevented the excessive accumulation of coal fines that may have blocked the fracture.

According to Figure 13d, in Experiment 3, under prolonged compaction, an increase in the uneven proportion of the two particle sizes led to a reduced final conductivity. A higher proportion of either large and medium particles or medium and small particles resulted in a lower conductivity. However, when the proportion of larger particles (either large or medium) reached five, there was a partial recovery in the conductivity. The greater presence of large particles corresponded to larger particle gaps, which could moderately improve the final conductivity.

This indicates that the proportions of large and small particles were the main factors influencing the conductivity of the propped fractures in the mentioned three experiments under different ratios. A higher proportion of large particles led to a stronger conductivity, while a higher proportion of small particles resulted in a poorer conductivity. However, maintaining a balance between the quantities of large and small particles based on this ratio was crucial. This ensured that the particle gaps could impede the excessive infiltration of the coal fines, while minimizing the impact on the final conductivity of the propped fractures.

Therefore, under the same closure pressure conditions and considering the long-term conductivity, the optimal choice is a composite proppant pack consisting of three particle sizes: 30/60/90 mesh (5:1:5), 30/60/90 mesh (3:1:3), or 30/60/90 mesh (5:1:3). These ratios should be evenly distributed, with a primary emphasis on large particles, followed by small particles, and medium particles as a supporting component. By employing this particle size distribution for the propped fractures, it can effectively fill the near-wellbore-opening fractures and far-end sliding fractures, preventing the closure of distant fractures and maximizing the CBM production, while minimizing the damage caused by the coal fines to the conductivity of the propped fractures.

It can be observed that, under the same closure pressure, after laying down a proppant pack with large particles, larger particle gaps were present. With an increasing compaction time, the fracture surfaces were continuously eroded, resulting in an increase in the coal fines content. These detached coal fines easily mixed into the particle gaps and accumulated in large quantities, leading to the blockage of the propped fractures and a severe impairment of their conductivity. To address this, it is necessary to increase the quantity of the small particles and adopt a mixed placement approach to balance the size of the particle gaps within the fracture. This ensures both the hindrance of excessive coal fines infiltration and a reduced impact on the final conductivity, achieving the goal of ratio optimization. It should be noted that, as the closure pressure increased, the compaction effect on the proppant pack became stronger, causing a reduction in the particle gaps. Therefore, a large quantity of small particles should be avoided to prevent gap blockage. Consequently, at low closure pressures, the proportion of small particles should be increased, while at high closure pressures, the proportion of small particles should be reduced, in order to achieve the effective conductivity of the propped fractures.

#### 4. Discussion

Table 3 shows the ranking of the short-term and long-term conductivity of the composite proppants in a coalbed. The conductivity tests in this study aimed to identify the impact of different gradations and ratios of composite proppants on the conductivity of propped fractures, rather than obtaining actual downhole conductivity. The observations from Table 3 indicate that, during the short-term conductivity, when the coal fines content was low, the impact on the conductivity can be disregarded. The conductivity of the composite proppant with mixed particle sizes was mainly influenced by the proportion of large or small particles. A higher proportion of large particles resulted in a stronger conductivity, whereas a higher proportion of small particles led to a weaker conductivity. This relationship was straightforward. However, during the long-term conductivity, coal fines were likely to be generated, and small particles could fill the gaps between the larger particles, hindering excessive coal fines infiltration and preventing fracture blockage. This

relationship was more intricate and challenging to manage. Nevertheless, based on the particle ratios in the table, the composite proppant with a particle ratio of 6:5 demonstrated the highest long-term conductivity, followed by the composite proppant with a particle ratio of 4:3.

**Table 3.** Ranking of conductivity for composite proppants with different particle size ratios.

Composite Proppant Ratio	Particle Ratio (Large:Medium:Small)	Short-Term Conductivity Ranking	Long-Term Conductivity Ranking
1:1:1	2:1	9	4
1:1:3	2:3	15	16
1:1:5	2:5	19	19
1:3:1	4:1	12	14
1:5:1	6:1	13	15
3:1:1	4:1	2	5
5:1:1	6:1	1	6
1:3:3	4:3	14	12
1:5:5	6:5	17	11
3:1:3	4:3	10	2
5:1:5	6:5	7	1
3:3:1	6:1	6	7
5:5:1	10:1	4	10
1:3:5	4:5	18	18
1:5:3	6:3	16	13
3:1:5	4:5	11	17
3:5:1	6:3	5	3
5:1:3	8:1	8	9
5:3:1	8:1	3	8

Therefore, based on the results of the conductivity tests, the following conclusions can be drawn: to achieve optimal long-term conductivity in coalbeds and considering the impact of coal fines, it is crucial to maintain a balanced proportion of large and small particles in composite propped fractures, with a focus on large particles. This approach guarantees sustained long-term conductivity and mitigates the excessive infiltration of coal fines and fracture blockage.

## 5. Conclusions

- (1) During the short-term conductivity in coalbed fracturing, the influence of coal fines on the conductivity of propped fractures can be neglected due to their low concentration. The conductivity decreases with an increase in the proportion of small particles. Under a closure pressure of 10 MPa, the conductivity of 30/60/90 mesh = 5:1:1 was  $59.9 \mu\text{m}^2\cdot\text{cm}$  higher than that of 1:1:5. A segmented and uniform placement approach, starting from the tip of the fracture and extending to the near-wellbore region, effectively filled the smaller-scale slip fractures in the distal region and the larger-scale opening fractures near the wellbore, thereby enhancing the conductivity.
- (2) In the long-term conductivity in coalbed fracturing, the continuous injection of proppants onto the coal rock fracture surface leads to an increase in coal fines concentration and a significant accumulation of proppant interstices, resulting in an impaired conductivity. To address this issue, it is necessary to appropriately increase the proportion of small particles and adopt a mixed placement approach to balance the particle interstices within the propped fracture. This approach prevents the excessive infiltration of coal fines, while minimizing the impact on long-term conductivity. After a compaction time of 70 h, the conductivity of 30/60/90 mesh = 5:1:5 was  $16.5 \mu\text{m}^2\cdot\text{cm}$  higher than that of 1:1:5.

- (3) In the current experiment, a mixed placement approach was used for the proppant particles, but the potential impact of particle crushing and subsequent particle interstice blockage due to the proppant particles' compaction on the conductivity of the proppant pack was not considered. In future studies, the influence of different placement methods on the conductivity and the impact of proppant compressive strength on the particle crushing rate should be taken into account to optimize the experimental results.

**Author Contributions:** Conceptualization, Q.C. (Qing Chen); methodology, Q.C. (Qing Chen); validation, Z.H.; formal analysis, Q.C. (Qing Chen) and X.K.; investigation, H.H., X.L. and F.X.; resources, H.H.; data curation, Q.C. (Qing Chen), H.H. and Q.C. (Qi Chen); writing—original draft preparation, Q.C. (Qing Chen); writing—review and editing, Q.C. (Qing Chen); supervision, X.K.; project administration, Z.H.; funding acquisition, Z.H. All authors have read and agreed to the published version of the manuscript.

**Funding:** This study was funded by the Sinopec Science and Technology Department Project-Key Volume-fracturing Technologies for middle-shallow tight sandstone Gas Reservoirs in West Sichuan (P22047) and PetroChina Chuanqing Drilling Engineering Co., Ltd., Optimization Design Technology and Field Test of Key Construction Parameters of Targeted Fracturing Temporary Plugging (CQCJ-2001-06).

**Data Availability Statement:** The raw/processed data required to reproduce the above findings cannot be shared at this time as the data also forms part of an ongoing study.

**Conflicts of Interest:** The authors declare no conflict of interest.

## References

1. Santiago, V.; Ribeiro, A.; Johnson, R., Jr.; Hurter, S.; You, Z. Modelling and economic analyses of graded particle injections in conjunction with hydraulically fracturing of coal seam gas reservoirs. *SPE J.* **2022**, *27*, 1633–1647. [[CrossRef](#)]
2. Chen, H.; Hu, W.; Liu, Q.; Tian, L.; Men, C.; Zhao, F. Optimization and Application of Segmental Fracturing Parameters for Low-Permeability and Ultra-Low-Permeability Coalbed Methane Horizontal Wells. *Coal Technol.* **2019**, *38*, 115–118.
3. Du, J.; Jiang, J.; Huo, Z.; Shen, Y. Quantitative Evaluation of Fracture Development and Permeability in High-Rank Coalbed Methane Reservoirs. *Coal Mine Saf.* **2019**, *50*, 181–184.
4. Wang, D.; You, Z.; Wang, M.; Li, Q.; Wu, L. Numerical investigation of proppant transport at hydraulic-natural fracture intersection. *Powder Technol.* **2022**, *398*, 117123. [[CrossRef](#)]
5. Wang, D.; You, Z.; Johnson, R., Jr.; Wu, L.; Bedrikovetsky, P.; Aminossadati, S.M.; Leonardi, C. Numerical investigation of the effects of proppant embedment on fracture permeability and well production in Queensland coal seam gas reservoirs. *Int. J. Coal Geol.* **2021**, *242*, 103689. [[CrossRef](#)]
6. Gao, C.; Ai, C.; Zhang, B.; Zhang, F. Analysis of Factors Affecting the Flow Conductivity of Coal-Rock Fractures. *Contemp. Chem. Ind.* **2015**, *44*, 1632–1633.
7. Palmer, I.; Moschovidis, Z.A.; Cameron, J.R. Coal Failure and Consequences for Coalbed Methane Wells. In Proceedings of the SPE Annual Technical Conference and Exhibition, Dallas, TX, USA, 9–12 October 2005.
8. Magill, D.P.; Ramurthy, M.; Halliburton; Jordan, R.; Devon; Nguyen, P. Controlling Coal-fines Production in Massively Cavitated Openhole Coalbed-methane Well. In Proceedings of the SPE Asia Pacific Oil and Gas Conference and Exhibition, Brisbane, QLD, Australia, 18–20 October 2010.
9. Cao, D.; Yuan, Y.; Wei, Y.; Liu, S.; Li, X.; Wang, Q. Comprehensive Classification Study of Coal Fines Genetic Mechanism and Origin Site. *Coal Geol. China* **2012**, *24*, 10–12.
10. Wei, Y.; Cao, D.; Yuan, Y.; Zhu, X.; Yao, Z.; Zhou, J. Characteristics and controlling factors of pulverized coal during coalbed methane drainage in Hancheng area. *J. China Coal Soc.* **2013**, *38*, 1424–1429.
11. Huang, F.; Dong, C.; Shang, X.; You, Z. Effects of proppant wettability and size on transport and retention of coal fines in proppant packs: Experimental and theoretical studies. *Energy Fuels.* **2021**, *35*, 11976–11991. [[CrossRef](#)]
12. Wen, Q.; Wang, Q. Analysis and Discussion on Factors Affecting the Long-Term Flow Conductivity of Proppants. *Inn. Mong. Petrochem. Ind.* **2003**, *3*, 101–104.
13. Hou, B.; Chen, M.; Wang, Z.; Yuan, J.; Liu, M. Hydraulic Fracture Initiation Theory for A Horizontal Well in A Coal Seam. *Pet. Sci.* **2013**, *10*, 219–225. [[CrossRef](#)]

14. Wang, M. Developmental Experiment and Numerical Simulation of Coal Bed Methane Considering the Effect of Coal Powder. Ph.D. Thesis, Southwest Petroleum University, Chengdu, China, 2016.
15. Wang, H.; Lan, W.; Liu, Y.; Zhang, H.; Yu, H. Mathematical model of fluid-solid coupling percolation with coal powder in coal reservoir. *Nat. Gas Geosci.* **2013**, *24*, 667–670.
16. Zhang, F.; Li, M.; Qi, Y.; Zhu, H.; Meng, S. Analysis of pulverized coal migration during CBM production. *J. China Univ. Pet.* **2015**, *39*, 86–92.
17. Li, Y.; Han, W.; Wang, Y.; Meng, S.; Wu, X.; Wang, Z.; Ma, Z.; Liu, D.; Zhao, S. Progress of coal fines agglomeration and settlement mechanism based on high efficiency coalbed methane drainage. *Coal Geol. Explor.* **2021**, *49*, 1–12.
18. Zheng, C.; Bao, J. Research on the Numerical Simulation for Migration Law of Pulverized Coal in Wellbore. *Unconv. Oil Gas* **2016**, *3*, 99–103.
19. Zhang, J.; Zhu, S.; Peng, X.; Deng, P. Tri-phase flow model of coalbed methane-water-solid and numerical simulation study. *China Offshore Oil Gas* **2022**, *34*, 117–127.
20. Liu, Y.; Zhang, S.; Cao, L.; Meng, S.; Zhang, T. Rules of coal powder migration and deposition in the proppant fracture. *J. China Coal Soc.* **2014**, *39*, 1333–1337.
21. Chen, W.; Wang, S.; Qin, Y.; Zhao, W.; Zhao, J.; Yang, J.; Li, R. Migration and control of coal powder in CBM well. *J. China Coal Soc.* **2014**, *39*, 416–421.
22. Zhao, S. Experimental Study on the Influence of Pore Structure on Seepage Characteristics in Tight Sandstone Reservoir. Master's Thesis, Xi'an Shiyou University, Xi'an, China, 2021.
23. Pan, L.; Zhang, S.; Zhang, J.; Lin, X. An experimental study on screening of dispersants for the coalbed methane stimulation. *Int. J. Oil Gas Coal Technol.* **2015**, *9*, 437. [[CrossRef](#)]
24. Yang, R.; Huang, Z.; Li, G.; Wei, Y.; Shen, Z. A semi-analytical method for modeling two-phase flow in coalbed methane reservoirs with complex fracture networks. *SPE Reserv. Eval. Eng.* **2018**, *21*, 719–732. [[CrossRef](#)]
25. Liu, Y.; Ouyang, W.; Zhao, P.; Lu, Q.; Fang, H. Numerical well test for well with finite conductivity vertical fracture in coalbed. *Appl. Math. Mech.* **2014**, *35*, 729–740. [[CrossRef](#)]
26. Huang, F.; Dong, C.; You, Z.; Shang, X.; You, Z. Detachment of coal fines deposited in fracturing proppants induced by single-phase water flow: Theoretical and experimental analyses. *Int. J. Coal Geol.* **2021**, *239*, 103728. [[CrossRef](#)]
27. You, Z.; Wang, D.; Leonardi, C.; Johnson, R., Jr.; Bedrikovetsky, P. Influence of elastoplastic embedment on CSG production enhancement using graded particle injection. *APPEA J.* **2019**, *59*, 310–318. [[CrossRef](#)]
28. Cao, K.; Jiang, J.; Guo, L.; Wang, L.; Ma, F.; An, D. Experimental Study on Flow Conductivity of Quartz Sand and Ceramic Composite Proppant. *Oil Drill. Prod. Technol.* **2016**, *38*, 684–688.
29. Li, Y.; Jia, D.; Gao, R.; Gao, C.; Mi, J.; Ai, C. Experimental Study on Long-Term Flow Conductivity of Complex Fractures in Coal and Rock. *Nat. Gas Oil* **2017**, *35*, 11+12+94–99.
30. Liang, T.; Cai, B.; Meng, C.; Zhu, X.; Liu, Y.; Chen, F. Influence of Hydraulic Fracturing Proppant Performance on Flow Conductivity. *Fault-Block Oil Gas Field* **2021**, *28*, 403–407.
31. Zhao, Z.; Wang, D.; Wang, G. Experimental Study on Long-Term Flow Conductivity Variation of Quartz Sand Proppant. *Drill. Prod. Technol.* **2022**, *45*, 72–77.
32. Jin, P.; Wang, X.; Zhang, S.; Wang, L.; Lu, Z. Analysis of Factors Affecting Flow Conductivity of Hydraulic Fracture in Tight Sandstone Reservoirs. *Fault-Block Oil Gas Field* **2022**, *29*, 234–238.
33. Chen, C.; Guo, J.; Lu, Q.; Ci, J. Study and Application of Multiscale Propping Mechanism in Tight Gas Reservoirs. *J. Southwest Pet. Univ.* **2022**, *44*, 131–138.
34. Zhu, H.; Zhao, F. Influence of Different Particle Size Combination Proppants on Flow Conductivity of Tight Sandstone Reservoirs. *Chem. Eng. Des. Commun.* **2022**, *48*, 27–29.
35. Zhang, H.; Wang, Y.; Yang, H. Study on Factors Affecting Flow Conductivity of Complex Fractures in Coalbed Methane Reservoirs. *Coal Mine Saf.* **2022**, *53*, 21–26.
36. Ren, L.; Hu, Z.; Zhao, J.; Lin, R.; Hu, D.; Li, Z.; Wu, J.; Peng, S. Optimization Design of Deep Shale Gas Fracturing Proppants Based on the Evaluation of Fracture Network Flow Efficiency. *Pet. Geol. Oilfield Dev. Daqing* **2023**, *42*, 148–157.
37. Xiao, F.; Zhang, S.; Li, X.; Wang, F.; Liu, X. Particle Size Combination and Slickwater Carrying Sand Placement Law and Flow Conductivity: A Case Study of Jimsar Shale Oil Reservoir. *Pet. Geol. Oilfield Dev. Daqing* **2023**, 1–8.
38. Wang, C.; Lu, Y.; Yi, X.; Qiu, X.; Dai, L.; Du, R.; Dong, L. Experimental Study on the Conductivity of Sand Filled Fractures in Coal and Rock. *Sci. Technol. Eng.* **2013**, *13*, 10604–10607+10612.
39. Zou, Y.; Zhang, S.; Zhang, J. Experimental Method to Simulate Coal Fines Migration and Coal Fines Aggregation Prevention in the Hydraulic Fracture. *Transp. Porous Media* **2014**, *101*, 17–34. [[CrossRef](#)]
40. Yang, Y.; Cao, Y.; Tian, H.; Li, D.; Zhang, H.; Sun, H.; Wu, X.; Chen, W. Mechanism analysis of coal fines damaged to coal reservoirs and prevention countermeasures during fracturing. *Coal Sci. Technol.* **2015**, *43*, 84–87.
41. Liu, Y.; Su, X.; Zhang, S. Influencing characteristics and control of coal powder to proppant fracture conductivity. *J. China Coal Soc.* **2017**, *42*, 687–693.

42. Ahamed, M.; Perera, M. Pressure-dependent flow characteristics of proppant pack systems during well shut-in and the impact of fines invasion. *J. Nat. Gas Sci. Eng.* **2021**, *96*, 104251. [[CrossRef](#)]
43. Liu, Z.; Wei, Y.; Zhang, Q.; Zhang, S.; Wang, A.; Cao, D. Physical simulation experiment of the effect of hydro chemical properties on the migration of coal fines in propped fractures. *J. China Coal Soc.* **2023**, 1–11.

**Disclaimer/Publisher's Note:** The statements, opinions and data contained in all publications are solely those of the individual author(s) and contributor(s) and not of MDPI and/or the editor(s). MDPI and/or the editor(s) disclaim responsibility for any injury to people or property resulting from any ideas, methods, instructions or products referred to in the content.